

# Conformational dependence of a protein kinase phosphate transfer reaction

Graeme Henkelman,<sup>1</sup> Montiago X. LaBute,<sup>1</sup> Chang-Shung Tung,<sup>1</sup> P. W. Fenimore,<sup>1</sup> and Benjamin H. McMahon<sup>1</sup>

<sup>1</sup>*Theoretical Division, Los Alamos National Laboratory, Los Alamos, New Mexico 87545*

(Dated: September 6, 2018)

Atomic motions and energetics for a phosphate transfer reaction catalyzed by the cAMP-dependent protein kinase (PKA) are calculated by plane-wave density functional theory, starting from structures of proteins crystallized in both the reactant conformation (RC) and the transition-state conformation (TC). In the TC, we calculate that the reactants and products are nearly isoenergetic with a 0.2 eV barrier; while phosphate transfer is unfavorable by over 1.2 eV in the RC, with an even higher barrier. With the protein in the TC, the motions involved in reaction are small, with only  $P_\gamma$  and the catalytic proton moving more than 0.5 Å. Examination of the structures reveals that in the RC the active site cleft is not completely closed and there is insufficient space for the phosphorylated serine residue in the product state. Together, these observations imply that the phosphate transfer reaction occurs rapidly and reversibly in a particular conformation of the protein, and that the reaction can be gated by changes of a few tenths of an Å in the catalytic site.

PACS numbers:

## INTRODUCTION

Protein kinases regulate many biological processes by transferring a phosphate group from adenosine triphosphate (ATP) to the sidechains of particular serine, threonine, or tyrosine residues. The bulky, charged phosphate group alters the conformation and function of the target protein [1, 2]. Different kinases recognize different primary sequence motifs surrounding the residue to be phosphorylated, in a highly regulated fashion [3, 4, 5, 6]. Structural studies have revealed several conformational changes, such as closing of the active-site cleft, the packing of the activation loop, and rotation of the C-helix, which are often implicated in controlling the activity of protein kinases [2]. The reasons for such control are clear, but no answer has been provided to such questions as: “How closed is closed?”, or “is this particular conformation of the activation loop ‘good enough’ for phosphorylation to occur?” Quantum chemistry is required to objectively answer these questions.

The extent of conformational heterogeneity in a covalent protein reaction was first quantified in a series of experiments monitoring the temperature-dependent re-binding of CO to myoglobin after flash photolysis [7]. Agmon and Hopfield created a concise phenomenological model describing this situation, using transition state theory to describe the vibrational reaction, and a diffusive coordinate which describes the protein conformation and modulates the reaction barrier to the vibrational transition [8, 9]. Moving beyond the phenomenological model requires specifying both the conformational heterogeneity and the sensitivity of the reaction barrier to this heterogeneity. Careful structural analysis [10] and quantum chemistry calculations [11] showed that the reaction barrier heterogeneity is indeed a reasonable consequence of observed structural heterogeneity at the myoglobin active site. A reevaluation of a wide variety of

myoglobin data also shows that a distinction between diffusive, solvent-controlled conformational motions and Arrhenius transitions which are independent of the solvent dynamics is well supported by experiments [12].

In this work, we explore the conformational sensitivity of the protein kinase reaction in two experimentally determined structures of PKA, one crystallized with ATP and the protein kinase inhibitor (PKI), which we refer to as the reactant conformation of PKA, or RC [13]. The other conformation is obtained by crystalizing with a transition-state analogue, a non-reactive ADP-AlF<sub>3</sub> and a mimic of PKI which is both shorter and has a phosphate-accepting serine instead of an inert alanine at the reactive position [14]. We refer to the protein conformation in this case as the transition state conformation of PKA, or TC. Although differences in conformation between the two structures are  $\sim 0.5$  Å, we find qualitatively different energetics of reaction, which lead us to conclude that conformational motion of the protein kinase is rate-limiting to the overall phosphate transfer reaction.

## METHODS

Initial equilibrium geometries are generated from the protein data bank entries 1ATP, (RC) and 1L3R, (TC), both crystal structures of PKA. Initial guesses for the complete reactant and product structures were obtained by homology-modeling the terminal phosphate of ATP ( $P_\gamma$ ) and side chains of the serine and catalytic aspartic acid (D-166) into appropriate positions. All atoms which were modeled in this way were allowed to move in subsequent geometry optimization steps. Four different model sizes, containing 82, 88, 244 and 263 atoms, were constructed. The 82-atom minimal system has been defined by Valiev *et al.* [15], and includes the Mg<sub>2</sub>-tri phosphate

and its immediate interaction partners, G-52, S-53, K-72, D-166, K-168, N-171, D-184, and the substrate serine residue. Two water molecules from the crystal structure are included to complete the six-fold coordination of Mg in the 88-atom system. The 244-atom system contains a significantly larger shell around the reaction center and more of the ATP molecule (including part or all of residues G-52, S-53, F-54, K-72, D-166, L-167, K-168, P-169, E-170, N-171, D-184, F-185, G-186, and the substrate backbone from residue 18 to 22). The atomic coordinates of backbone carbon and nitrogen atoms for each system were taken directly from the experimental crystal structures. Non-backbone bond lengths and most angles are derived from amino acid templates to facilitate comparison of energies between structures. Protons were added where needed. Residues were truncated by replacing carbon atoms with protons and adjusting the new C-H bond length accordingly. Full atomic coordinates are provided in the supporting material.

Atomic interactions are described by the VASP density functional theory (DFT) and a plane waves basis [16, 17]. Ultrasoft pseudopotentials of the Vanderbilt form [18], and a PW91 generalized gradient approximation functional are used. A 270 eV plane wave cutoff, appropriate for the pseudopotentials, is applied. This cutoff was increased to 300 eV to verify insensitivity of results to choice of basis set. The reaction pathways are computed with periodic images separated by at least an 8 Å vacuum layer. A periodic box size of  $19 \times 21 \times 16 \text{ \AA}^3$  is used for the 82- and 88-atom clusters,  $20 \times 24 \times 21 \text{ \AA}^3$  for the 244-atom cluster and  $27 \times 24 \times 23 \text{ \AA}^3$  for the 263 atoms structure.

Reactant and product geometries are calculated by optimizing the geometry of the clusters with a conjugate gradients algorithm. Saddle points connecting these stable geometries were found using the nudged elastic band (NEB) method [19]. In this method, images are generated by linear interpolation between the optimized reactant and product structures, and DFT is used to calculate forces on each atom of each image. The images are then geometry optimized subject to harmonic forces between the images which force them to be equally spaced along a minimum energy pathway between reactants and products. The climbing image modification to the NEB method [20, 21] was used so that the highest energy image along the band converges directly to the saddle point, thus increasing the accuracy of the energy barrier with **fewer images**. Refinements to the barriers for small system changes were computed with the dimer saddle point finding method [22].

The 82-atom system contains the same 59 unconstrained atoms as Valiev *et al.*, while the waters added to make the 88-atom system were allowed to move. The 244-atom system has only 42 moving atoms (the gamma phosphate, Mg1, Mg2, their coordinated water, and the sidechains of S-21, D-166, and K-168).

In order to test the sensitivity of the 244-atom result to system size changes and details of the electrostatic boundary conditions and periodic box size, we added the adenosine ring to make a 263 atom system, and observed changes to the barrier for TC of less than 15 meV.

## RESULTS

### conformational dependence

Fig. 1a shows the energetics of the 244-atom systems. The reaction is endothermic in RC by 1.2 eV, while in TC, the reaction is nearly isoenergetic with a barrier of only 0.20 eV. The reaction pathway of TC, shown in Fig. 1b, shows only small motions during the reaction; only two atoms move more than 0.5 Å, and the catalytic base moves only 0.07 Å. Apparently, in the TC structure, the atoms around the active site are correctly arranged for both the reactants and products state. In contrast, 1.2 eV endothermicity in RC indicates sub-optimal geometries in the product state.

At the transition state, the  $P_\gamma O_3$  has a planar configuration, halfway between the ADP and the serine  $O_\gamma$ , and proton transfer from the serine to the Asp-166 occurs after the phosphate transfer. Transferring the proton to an oxygen atom on the  $P_\gamma$  phosphate was found to be unfavorable by more than 0.5 eV. These observations are in agreement with previous DFT studies [15].

One possible spurious origin for the low barrier in TC is that both the reactants and products are destabilized because the active site has collapsed around the  $AlF_3$ , just as we expect RC to be energetically biased towards the reactants. Two observations force us to the conclusion that this is not occurring.

Examination of the reaction pathway geometries reveals two clear reasons for the endothermicity in the TC structure. First, the reaction cleft in RC is approximately 1 Å more open in RC than in TC, so the protein is unable to maintain the full octahedral coordination of both magnesium ions in the products state. Fig. 2 shows this distance between the N-171 oxygen and the closest  $P_\beta$  oxygen to be 5.1 Å in the RC conformer. In the TC structure, the reaction center is compressed, reducing this distance to 4.2 Å. Second, it appears that there is more space for the phosphorylated serine residue in TC than RC.

Fig. 1a maintains the relative energies of RC and TC, and shows that TC is only 160 meV higher than RC. The errors contributing to this difference are likely several tenths of an eV, but it is gratifying that the reactants energies are so similar in the two conformations.

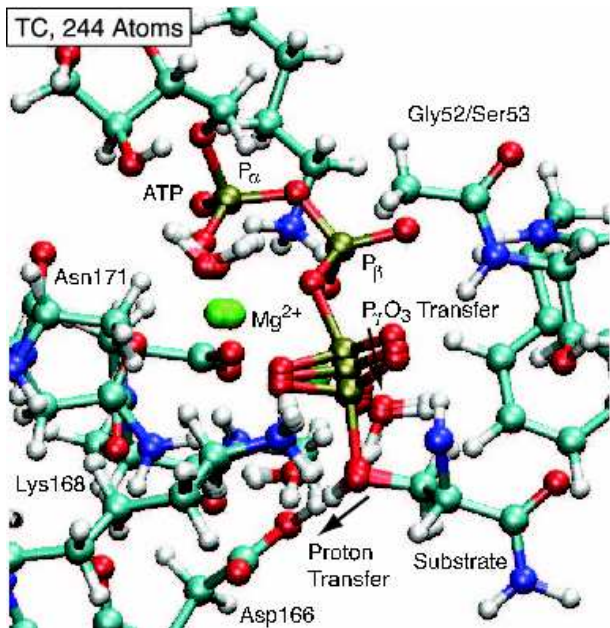
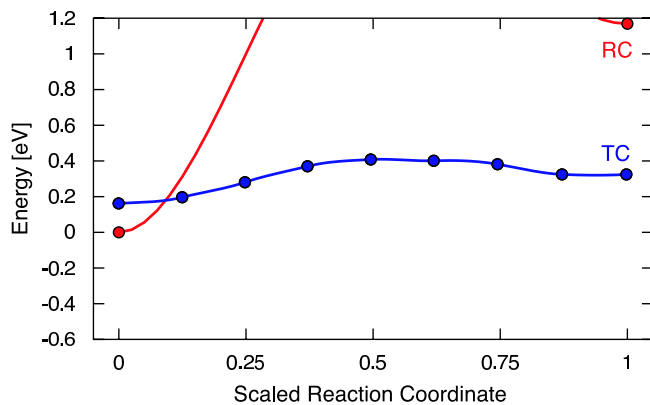


FIG. 1: (a) Energy barrier for the 244-atom system in the RC and TC conformers. With the additional constraining atoms, the RC reaction becomes very unfavorable, while the TC conformation phosphorylates. (b) Reaction path for phosphate transfer in PKA for a 244-atom TC structure. The additional constraining atoms on the outside of the cluster, as compared to the 82-atom system in Fig. 3(a), reduce spurious motion during the reaction. For example, the central  $Mg^{2+}$  ion remains in place with the proper coordination throughout this reaction.

### geometry constraints

Another question arises from the relatively small set of moving atoms allowed in the calculation shown in Fig. 1. One might expect the geometry-optimized reaction pathway to be independent of initial conformation in the limit of the entire protein being allowed to move. Several observations force us to the conclusion that this is not correct.

First, energetic minimization of both RC and TC towards the reactants state, using a classical molecular dynamics potential (which should be perfectly valid for the

	82 RC	244 RC	82 TC	244 TC
Mg1	0.63	0.16	0.61	0.10 (0.04)
Mg2	1.07	1.04	0.42	0.25 (0.16)
$P_\gamma$	1.65	1.10	1.20	0.89 (0.56)
$O_{1\gamma}$	1.20	0.53	0.72	0.35 (0.22)
$O_{2\gamma}$	1.43	0.67	0.64	0.33 (0.19)
$O_{3\gamma}$	0.99	0.42	0.56	0.49 (0.37)
Ser $O_\gamma$	1.43	0.43	1.52	0.27 (0.25)
H	1.24	1.35	1.25	0.53 (0.07)
Asp O	1.12	0.57	0.96	0.07 (0.04)

TABLE I: The distances in Å that particular atoms moved in the four reaction pathways. The distance from the reactants minimum to the transition state is indicated in parenthesis for the 244-atom TC structure.

reactants state) causes only one third of the difference in the distance shown in Fig. 2 to disappear, even with no solvent present and every atom in the protein allowed to move during the optimization.

Second, Table I, shows much smaller motions are needed for reaction in TC than in RC. The  $Mg^{++}$  ions, coordinated water molecules, catalytic base, and lysine all move  $\sim 0.1$  Å in TC, and 0.5 to 1.0 Å in RC. Even the serine residue, which gains a phosphate group, moves only a quarter Å during the course of reaction. A related observation is that the change in force on the frozen atoms during reaction is about half as large for TC than RC (not shown).

To directly check the effect of constraint on the results, and guided by knowledge of the forces on frozen atoms, we relieved the constraint on the beta phosphate of ATP. The relative energy of RC and TC went up by 350 meV, while the maximum change in force dropped by a factor of ten, and was uniformly distributed across a dozen boundary atoms. The exothermicities of RC and TC changed by less than 0.1 eV, while optimal geometries differed by  $\sim 0.1$  Å, suggesting that the templates used to build the Mg-triphosphate coordination sphere differed from the quantum mechanical potential by  $\sim 0.1$  Å in several places.

The conclusion that TC provides a structure with happy reactants as well as the potential to create happy products with minimal motions is robust.

### dependence on system size

Valiev et al. [15] reported a barrier of 0.5 eV for this reaction, when using either a GGA or B3LYP functional and local basis set on an 82-atom version of the RC structure, with only a pair of atoms fixed at the boundary of each molecular fragment. This result is intermediate between our RC and TC results, and could indicate



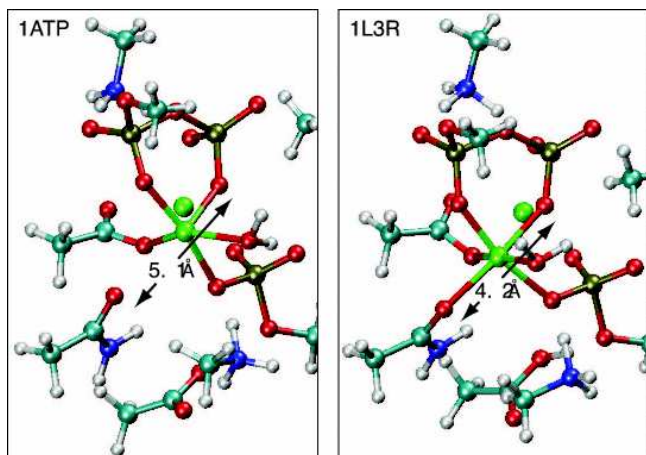


FIG. 2: The 82-atom system in the TC structure has a lower barrier than the RC structure and a favorable product state because the reaction center is compressed. In the product and transition states, the central Mg atom can remain octahedrally coordinated in the TC conformer. In the RC conformer the reaction cleft is opened and the same Mg atom is forced to break one bond, making the reaction unfavorable. The distance between the coordinating oxygen atoms on the Asn171 and ADP groups, which is a measure of reaction center size, is increased from 4.3 Å in the TC structure to 5.0 Å in the RC structure.

computational details provide variability as large as the conformational differences which we cite.

To check this possibility, we duplicated their 82-atom system and choice of constraints, and show the results of our calculation in Fig. 3, for both RC and TC. Consistent with their result, we find a 0.5 eV barrier and an exothermicity of 0.2 eV in the RC, indicating a robustness of the result to the various truncation procedures, basis sets, periodic boundary conditions, and functionals used the calculations. Unfortunately, the result is also insensitive to the starting conformation of the protein, in contrast to the results on the 244-atom systems.

Table I shows that the motions of the atoms are much larger than in the 244-atom calculation, and comparison of Figs. 1b and 3b shows a qualitatively larger and more contorted reaction dynamics in the smaller system. Further reflection suggests that atoms are moving that would not be able to in the complete protein system, for example the  $Mg^{2+}$  ions. We tested this by adding two crystallographic water molecules to  $Mg_1$ , and observing the reaction to become endothermic by  $\sim 0.5$  eV. Clearly, the 82-atom system is under-constrained because it is not large enough to provide accurate energetics of the relative reaction rate of the two systems.

A potentially very useful observation is that the geometries of reaction in the 82-atom calculation for both conformations share several similarities with the 244-atom TC calculation. This suggests that the underconstrained calculations can offer useful clues as to which conforma-

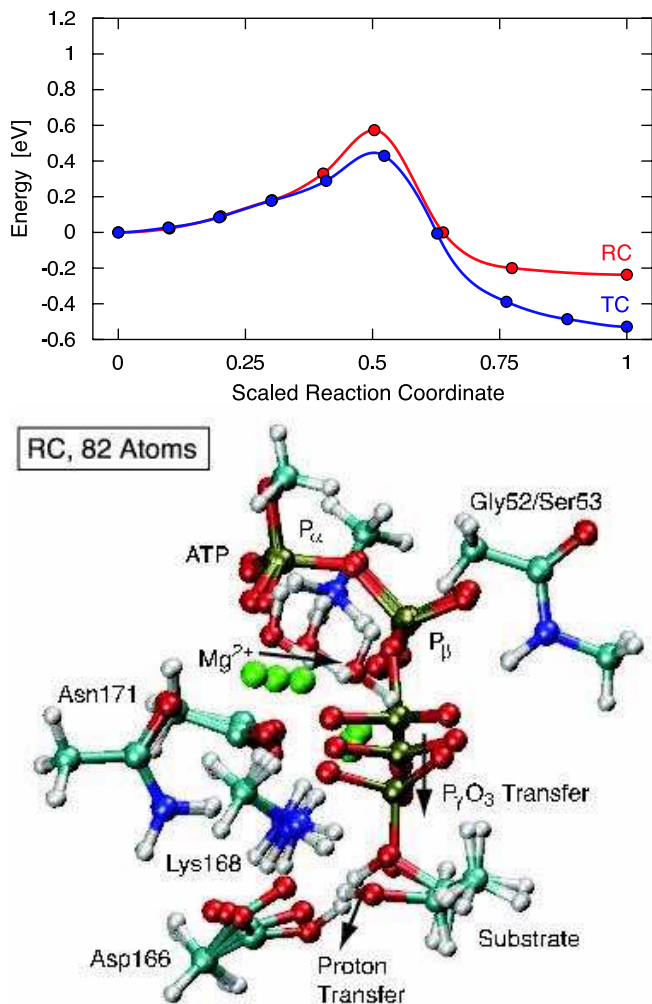


FIG. 3: (a) Energy barrier for the 82-atom system in the RC and TC structures. The TC transition state analog lowers the reaction barrier and favors the product state. The TC energies are shifted down by 400 meV relative to the RC energies to facilitate comparison. Each circle represents an image in the NEB calculation. (b) Reaction path for phosphate transfer in RS PKA with 82 atoms. The three image sequence is the reactant state, transition state, and product state. The atoms are color-coded: Red is oxygen, light blue is carbon, dark blue is nitrogen, silver is hydrogen, green is magnesium and gold is phosphorus. At the transition state the phosphate group is planar and the substrate proton has not yet transferred to the Asp166 catalytic base.

tions will favor reaction.

An energetic offset of 400 meV has been subtracted from TC for ease of comparison of the barrier and exothermicity to RC. Although we do not place great confidence in this number, it is interesting to note that the additional interactions included in the 244-atom system stabilize the reactive conformation of the protein.

## DISCUSSION

Much has been written about the reaction dynamics problem [23, 24, 25, 26], but it is primarily concerned with the very difficult problem of combining the vibrational transition with solvent motions. These ideas lead to something like [27], which does not make use of the separation of energy scales which comes from understanding protein dynamics, *per se*, and does not provide modularity of the different aspects of the calculation (quantum mechanical, hydration, and conformational motions.) By allowing relatively few atoms to move, we increase the probability that the dynamics of traversing our zero-temperature pathway will be simple enough to occur quickly. The formalism of Agmon and Hopfield can then be used to relate the vibrational transition to an overall reaction rate.

The current calculations are evaluated in the context of the Agmon-Hopfield model in Figure 4a, which shows the 1ATP (RC) structure at the peak of a distribution of conformations and 1L3R (TC) at the side. Figure 4b shows the barrier computed in the two calculations —  $60 k_B T$  for the reactant conformer and  $6 k_B T$  for the transition conformer. Figure 4c shows the reaction flux across the barrier as a function of protein conformation, simply the product of the probability of a conformation with the rate of reaction for that conformation  $g(cc)k(cc)$ , where  $k(cc) = \exp[-H(cc)/k_B T]$ .

This model provides an estimate of the distance-scale over which the barrier changes can be made by combining the information in Figs. 2 and 4c, which shows that a  $0.9 \text{ \AA}$  shift in the  $\text{Mg}^{2+}$  position, combined with several other changes of a similar size shifts the barrier by  $50 k_B T$ . Thus, a reasonable flux is confined to a multi-dimensional region only  $\sim 0.2 \text{ \AA}$  wide! Allostery is the property by which small molecules or proteins binding distant from the active site can influence activity by changing the protein conformation; the present calculation shows that these changes can be quite subtle.

The exact value of the reaction rate requires knowledge of the conformational occupancy of the low-barrier conformation, which we have not attempted to calculate in this work. There is a need for methods that can explore conformational changes in proteins. In this regard, inspection of the calculation in Fig. 3 can be quite helpful in discovering what conformations to look for when screening an MD simulation to find the correct portion of conformation space.

A recent crystal structure of a Y204A mutation of PKA in complex with a peptide inhibitor supports two aspects of our calculation [28]. First, a mixture of reactants and products can co-exist, and second, very few residues move in the course of the phosphate transfer. Yang *et al.* specifically note the absence of motion in the  $\text{Mg}^{++}$  ions, coordinated water, K168, and S53 [28].

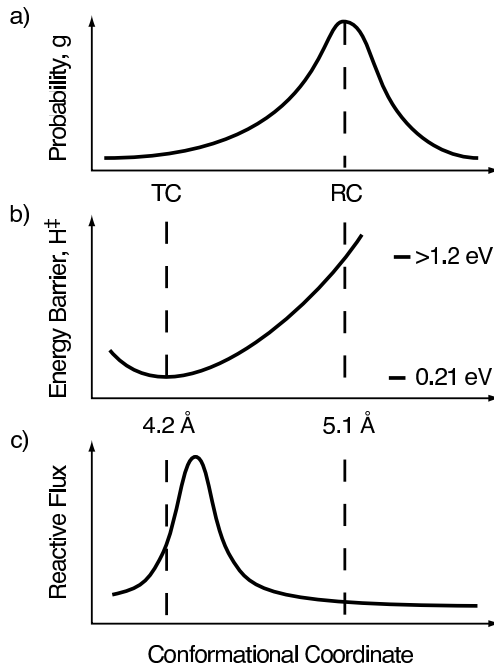


FIG. 4: Schematic separation of reaction rate into conformational and vibrational (Arrhenius) coordinates. (a), The distribution of protein conformations, with RC representing an average structure and TC a less-populated member of the distribution. (b) We have calculated an enthalpy barrier for two members of the ensemble, and interpolated between in this figure. (c) Reactive flux as a function of conformation, calculated using the Agmon-Hopfield formalism, described in the text.

## CONCLUSIONS

Two important lessons can be learned from this work. First, approximately 200 atoms need to be included to obtain the correct electronic structure, and also maintain enough constraints on the boundary conditions to meaningfully reproduce the effect of protein conformation on reaction rate. Second is the existence of the zero-temperature pathway in this particular case. In proteins where it is not possible to obtain TC crystal structures, it is essential to find appropriate methods to explore the variety of protein conformational motions. Since protein motions typically occur on timescales ranging from hundreds of nanoseconds to microseconds, it is unlikely that simple embedding of the quantum region in a larger classical region will resolve this difficulty.

Is *ab-initio* quantum chemistry now in a position to answer the biologically motivated questions posed in the introduction? It is clear, at least, that the active site cleft is **not** closed far enough in the RC structure. On the other hand, the real power of these techniques will only become evident when it is possible to thoroughly sample conformational motions of proteins and protein complexes. If studies of protein folding are any guide,

this day is fast-approaching [29].

## ACKNOWLEDGMENTS

We thank Matt Challacombe, Angel García, John Portman, Art Voter, and Hans Frauenfelder for valuable discussions and Matt Challacombe for obtaining the necessary computer time on the QSC supercomputer at Los Alamos National Lab, which made the large simulations possible. GH would also like to acknowledge Eric Galburt for suggesting that the NEB method should be used to look at reaction mechanisms in biological systems [30]. This work was performed with support from the Department of Energy, under contract W-7405-ENG-36 and the Laboratory Directed Research and Development program at Los Alamos National Laboratory.

- 
- [1] C.M. Smith, E. Radzio-Andzelm, Madhusudan, P. Akamine, and S.S. Taylor, "The catalytic subunit of cAMP-dependent protein kinase: prototype for an extended network of communication" *Progress in Biophys. and Mol. Bio. BIOLOGY* **71**:313-341 (1999).
  - [2] L.N. Johnson and R.J. Lewis, "Structural basis for control by phosphorylation" *Chemical Reviews* **101**:2209–2242 (2001).
  - [3] R.B. Pearson and B.E. Kemp "Protein-kinase phosphorylation site sequences and consensus specificity motifs – tabulations" *Methods in Enzymology* **200**:62–81 (1991).
  - [4] Z. Songyang, K.P. Lu, Y.T. Kwon, L.H. Tsai, O. Filhol, C. Cochet, D.A. Brickey, T.R. Soderling, C. Bartleson, D.J. Graves, DJ, et. al. "Structural basis for substrate specificities of protein Ser/Thr kinases: Primary sequence preference of casein kinases I and II, NIMA, phosphorylase kinase, calmodulin-dependent kinase II, CDK5, and Erk1" *Mol. and Cell. Biol.* **16**:6486-6493 (1996).
  - [5] Pinna, L. A. and M. Ruzzene, "How do protein kinases recognize their substrates" *Biochimica et Biophysica Acta* **1314**:191-225 (1996).
  - [6] R.I. Brinkworth, R.A. Breinl, and B. Kobe, "Structural basis and prediction of substrate specificity in protein serine/threonine kinases" *PNAS USA* **100**:74–79 (2003).
  - [7] R.H. Austin, K.W. Beeson, L. Eisenstein, H. Frauenfelder, and I.C. Gunsalus "Dynamics of ligand binding to myoglobin" *Biochem.***14**:5355–5373 (1975).
  - [8] N. Agmon, J. J. Hopfield "Transient kinetics of chemical reactions with bounded diffusion perpendicular to the reaction coordinate - intramolecular processes with slow conformational-changes" *J. Chem. Phys.* **78**, 6947–6959 (1983).
  - [9] N. Agmon, J. J. Hopfield, "CO binding to heme-proteins - a model for barrier height distributions and slow conformational changes" *J. Chem. Phys.* **79**, 2042–2053 (1983).
  - [10] J. Vojtechovsky, K. Chu, J. Berendzen, R. M. Sweet, I. Schlichting "Crystal structures of myoglobin-ligand complexes at near-atomic resolution " *Biophys. J.* **77**, 2153–2174 (1999).
  - [11] B. H. McMahon, B. P. Stojkovic, P. J. Hay, R. L. Martin, A. E. García, "Microscopic model of carbon monoxide binding to myoglobin" *J. Chem. Phys.* **113**, 6831-6850 (2000).
  - [12] P. W. Fenimore, H. Frauenfelder, B. H. McMahon, and F. G. Parak, "Slaving: Solvent fluctuations dominate protein dynamics and functions " *PNAS USA* **99**, 16047 (2002).
  - [13] J. Zheng, D. R. Knighton, L. F. Ten Eyck, R. Karlsson, N.-h Xuong, S. S Taylor, and J. M. Sowadski "Crystal structure of the catalytic subunit of camp-dependent protein-kinase complexed with MgATP and peptide inhibitor" *Biochemistry* **32**, 2154 (1993).
  - [14] Madhusudan, P. Akamine, N.H. Xuong, S.S. Taylor "Crystal structure of a transition state mimic of the catalytic subunit of cAMP-dependent protein kinase" *Nature Str. Biol.* **9**:273–277 (2002).
  - [15] M. Valiev, J. H. Weare, J. A. Adams, and R. Kawai "The role of the putative catalytic base in the phosphoryl transfer reaction in a protein kinase: First-principles calculations" *J. Amer. Chem. Soc.* **125**:9926-9927 (2003).

- [16] G. Kresse and J. Hafner, Phys. Rev. B **47**, 558 (1993); **49**, 14251 (1994).
- [17] G. Kresse and J. Furthmüller, Comput. Mater. Sci. **6**, 16 (1996); Phys. Rev. B **54**, 11169 (1996).
- [18] D. Vanderbilt, Phys. Rev. B **41** 7892 (1990).
- [19] H. Jónsson, G. Mills, and K. W. Jacobsen, in *Classical and Quantum Dynamics in Condensed Phase Simulations*, edited by B. J. Berne, G. Ciccotti, and D. F. Coker (World Scientific, Singapore, 1998).
- [20] G. Henkelman and H. Jónsson, J. Chem. Phys. **113**, 9978 (2000).
- [21] G. Henkelman, B. P. Uberuaga, and H. Jónsson, J. Chem. Phys. **113**, 9901 (2000).
- [22] G. Henkelman and H. Jónsson, J. Chem. Phys. **111**, 7010 (1999).
- [23] A. Warshel “Computer simulations of enzyme catalysis: Methods, progress, and insights” *Ann. Rev. Biophys. Biomol. Str.* **32**:425–443 (2003).
- [24] P. Hanggi, P. Talkner, M. Borkovec “Reaction-rate theory - 50 years after Kramers” *Rev. Mod. Phys.* **62**:251–341 (1990).
- [25] H. Frauenfelder and P.G. Wolynes “Rate theories and puzzles of hemeprotein kinetics” *Science* **229**:337-345 (1985).
- [26] C. Zheng, V. Makarov, and P.G. Wolynes “Statistical survey of transition states and conformational substates of the sperm whale myoglobin-CO reaction system” *J. Am. Chem. Soc.* **118**:2818–2824 (1996).
- [27] J. Florian, M.F. Goodman, A. Warshel “Computer simulation of the chemical catalysis of DNA polymerases: Discriminating between alternative nucleotide insertion mechanisms for T7 DNA polymerase” *J. Am. Chem. Soc.* **125**:8163–8177 (2003).
- [28] Yang, J; Ten Eyck, LF; Xuong, NH; Taylor, SS “Crystal structure of a cAMP-dependent protein kinase mutant at 1.26 angstrom: New insights into the catalytic mechanism” *J. Mol. Biol.* **336**:473-487 (2004).
- [29] Clementi, C; Garcia, AE; Onuchic, JN “Interplay among tertiary contacts, secondary structure formation and side-chain packing in the protein folding mechanism: All-atom representation study of protein L” *J. Mol. Biol.* **326**:933–954 (2003).
- [30] E.A. Galburt and B. L. Stoddard, Physics Today **54**, 33 (2001).



